DOI 10.1515/secm-2012-0045 — Sci Eng Compos Mater 2012; 19(4): 387–391

Li Wei*, Shan Shaofu and Fang Qianghan

Surface properties of the *in situ* formed ceramic-reinforced composite coating on TA15 alloy

Abstract: A hard composite coating was fabricated by laser alloying of the Co-Fe-Al+B_4C-Si_3N_4 mixed powders on TA15 (Ti-6Al-2Zr-1Mo-1V) titanium alloy in an open system. The composite coating mainly consisted of γ-Co, TiB_2, TiB, $TiC_{0.3}N_{0.7}$, SiC, Ti_3Al, FeAl, and Co-Ti intermetallics. The TEM diffraction pattern results indicated that the orientation relationship between TiB_2 and $TiC_{0.3}N_{0.7}$ was $(1\bar{}20)TiB_2//(2\bar{}20)TiC_{0.3}N_{0.7}$ in such a coating. Furthermore, during the alloying process, a number of Mo and Zr entered into the molten pool from the substrate due to the dilution effect, which refined the microstructures of the composite coating and also increased the amorphous phase content.

Keywords: composites; sliding wear; TA15 titanium alloy.

***Corresponding author: Li Wei,** Mechanical Engineering Faculty, Laboratory of Metal Technology, Shandong Jiao'tong University, Jinan 250023, China, e-mail: obinnali@126.com
Shan Shaofu: Mechanical Engineering Faculty, Shandong Jiao'tong University, Jinan 250023, China
Fang Qianghan: Mechanical Engineering Faculty, Laboratory of Metal Technology, Shandong Jiao'tong University, Jinan 250023, China

1 Introduction

TA15 (Ti-6Al-2Zr-1Mo-1V) titanium alloy is an important material, which has been extensively used in the aircraft industry. It is a near α titanium alloy, which was developed as BT20 titanium alloy by the former USSR [1]. Laser alloying is a promising technique for improving the wear, fatigue, and corrosion resistance of the machine titanium alloys [2].

Titanium borides have an excellent wear resistance, and the composite coatings containing the titanium borides have been observed on titanium alloys with different surface boronizing processing technologies. Moreover, Co-Ti or Fe-Al intermetallics also exhibited a lot of the good properties, such as excellent wear and high temperature resistance [3, 4]. SiC, TiB_2, and Ti(CN) are advanced ceramics that have been developed to satisfy the applications where the wear resistance and high strength are required [5, 6]. Laser alloying of the Co-Fe-Al+B_4C-Si_3N_4 pre-placed powders on TA15 titanium alloy substrates can form the ceramic-reinforced hard composite coating, which improved the resistance of the substrate. This paper will discuss the microstructures and wear properties of the Co-Fe-Al+B_4C-Si_3N_4 laser alloying composite coating on TA15 titanium alloys. This research provides essential theoretical and experimental basis to promote the application of laser alloying technology in the field of the surface modification.

2 Experimental

A 5-kW continuous CO_2 laser (TJ-HL-T5000) was used to prepare the alloying layer. The chemical compositions of TA15 alloy in this study are as follows (wt.%): 6.06Al, 2.08Mo., 1.32V, 1.86Zr, 0.09Fe, 0.08Si, 0.05C, 0.07O, and balance Ti. The pure TA15 samples (10 mm×10 mm×35 mm or 10 mm×10 mm×10 mm) were used in this research, and the thickness of the pre-placed layer was 0.7 mm. The alloying surfaces were ground with emery paper to remove the oxide scale and rinsed with alcohol before laser alloying. Alloy powders of Co (≥99.5% purity, 20~150 μm), Fe (≥99.5% purity, 50~150 μm), Al (≥98.5% purity, 50~150 μm), B_4C (≥99.5% purity, 50~200 μm), and Si_3N_4 (≥99.5% purity, 50~100 μm), were used for the laser alloying, and the water glass was used to be the binder to form a layer. Process parameters of laser alloying: laser power P=0.85~1.15 kW, scanning velocity V=3~7.5 mm/s, and the laser beam diameter D=4.5 mm. The diameter of the laser beam was obviously less than that of the width of the samples, so the four-track lap alloying layer was adopted in order to cover a whole alloying plane of the sample, and the lap rate was approximately 35%. During the laser alloying process, the surface oxidation was prevented by argon with a flow rate of 40 L/min. The compositions of the pre-placed powders used in this experiment were 20 wt.% Co+20 wt.% Fe+20 wt.% Al+30 wt.% B_4C+10 wt.% Si_3N_4. Before the laser alloying process, the pre-placed alloying powders should be mixed up until smooth, and the pre-placed alloying powder layer with the depth of 0.8 mm was smeared on the substrate; the water glass was used to be the binder.

The wear resistance of the composite coating was tested by SFT-2M disc wear tester. HV-1000 microsclerometer was used to test the microhardness of the composite coating. SMX-1000/1000L X-ray diffractometer (XRD) was used to determinate the phase constituent of the composite coating. The microstructural morphologies of the composite coating were analyzed by means of S-520 scanning electron microscope (SEM) and JEM-2010 high-resolution transmission electron microscope (HRTEM).

3 Results and analysis

3.1 XRD and SEM analysis

The XRD results indicated that this composite coating mainly consisted of γ-Co, TiB_2, TiB, $TiC_{0.3}N_{0.7}$, SiC, Ti_3Al, FeAl and Co-Ti intermetallics (see Figure 1). The XRD results also indicated that Ti_3Al, FeAl, TiB, TiB_2, $TiC_{0.3}N_{0.7}$, SiC, and Co-Ti intermetallics can be produced through the *in situ* metallurgical reactions during the laser alloying process. The production of Ti_3Al indicated that a Ti-rich molten pool was obtained during the alloying process, which was favorable to the production of TiB. In fact, the energy of the laser beam showed the Gauss distribution, the bottom of the molten pool absorbed less energy than those of the other locations. The different locations absorbed different amounts of energy, i.e., the middle of the coating absorbed more energy than the edge of the laser beam.

It was noted that the composite coating was metallurgically bonded to the TA15 substrate in the sample (see Figure 2A). As shown in Figure 2B, the $TiC_{0.3}N_{0.7}$ bulk shape and the Ti-B stick shape precipitates were dispersed uniformly in the matrix, which increased the microhardness of the composite coating, and the Ti-B compounds played an important role in refining the microstructure of the alloying coating. Moreover, due to the dilution effect of the substrate to the laser layer, a number of Mo entered into the alloying layer from the substrate. Mo and its compounds refined the microstructure of the composite coating, which played an important role in improving the wear resistance of the coating [7].

Owing to the rapid cooling rate of the molten pool, a small amount of elements, such as Si, B, and Mo had no time to precipitate from the liquid and solution in γ-Co to form a supersolution, which caused the solution strengthening. As shown in Figure 2C, the Ti-Co binary intermetallic alloy had uniform and dense microstructures consisting of the primary dendrites and a few interdendritic eutectic-like structures. In fact, the upper layer absorbed the most energy from the laser beam, so the crystals, such as Ti-B compounds and SiC took a long time to grow up, leading to the formation of the coarse structure (see Figure 2D).

3.2 Microstructure analysis

Figure 3A shows the structure of the test area in the alloying layer. Figure 3B is the composite electron diffraction pattern of TiB_2[001] and $TiC_{0.3}N_{0.7}$[332] zone axis. The diffraction pattern indicated that the orientation relationship between TiB_2 and $TiC_{0.3}N_{0.7}$ was $(\bar{1}20)TiB_2//(\bar{2}\bar{2}0)TiC_{0.3}N_{0.7}$. The HREM analysis result indicated that the SiC high-resolution lattice phase was produced in the alloying layer, which corresponded to its (103) crystal plane (see Figure 3C). The HREM analysis result indicated that the $Mo_5(Si, Al)_3C$ high-resolution lattice phase was produced in the alloying layer, which corresponded to its (310) crystal plane (see Figure 3D). The production of SiC-$Mo_5(Si, Al)_3C$ further refined the microstructures of the composite coating [8, 9].

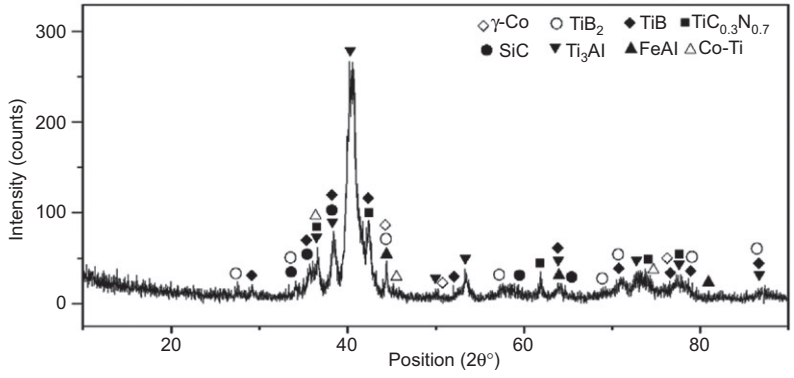

Figure 1 X-ray diffraction diagram of the Co-Fe-Al+B_4C-Si_3N_4 composite coating on TA15 titanium alloy.

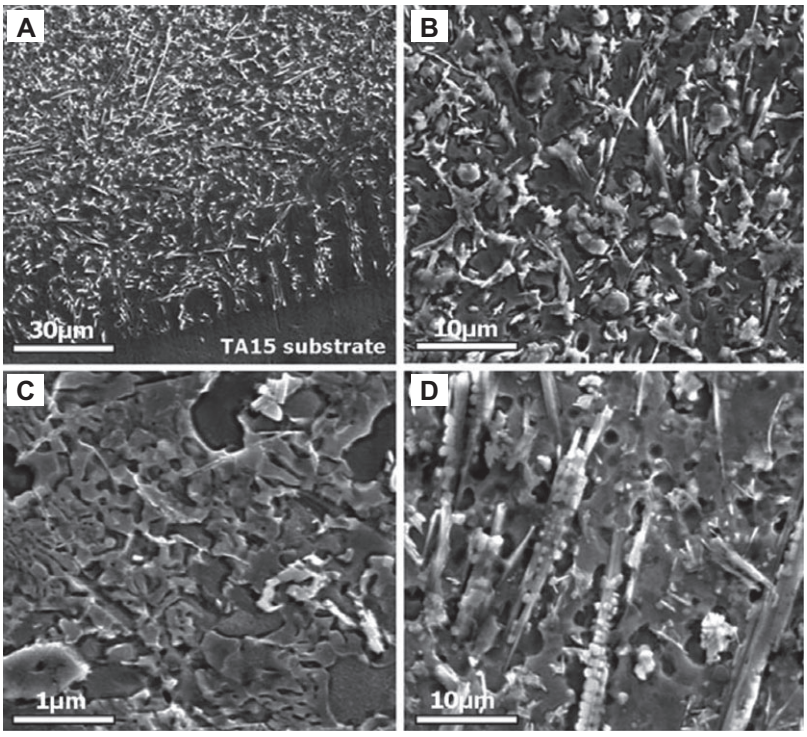

Figure 2 SEM micrographs of the composite coating in the sample, (A) the bonding zone, (B) the clad zone, (C) Ti-Co binary intermetallic alloy, and (D) microstructure.

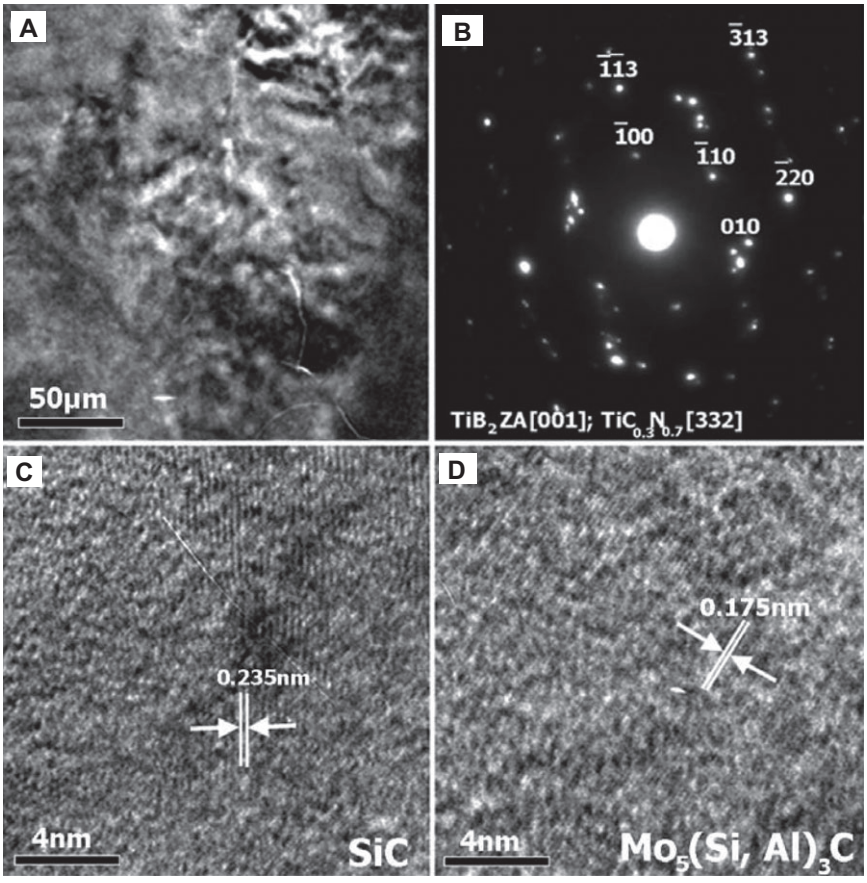

Figure 3 TEM micrographs (A), the diffraction pattern (B), the HREM morphologies of SiC (C), and $Mo_5(Si, Al)_3C$ (D) in the composite coating.

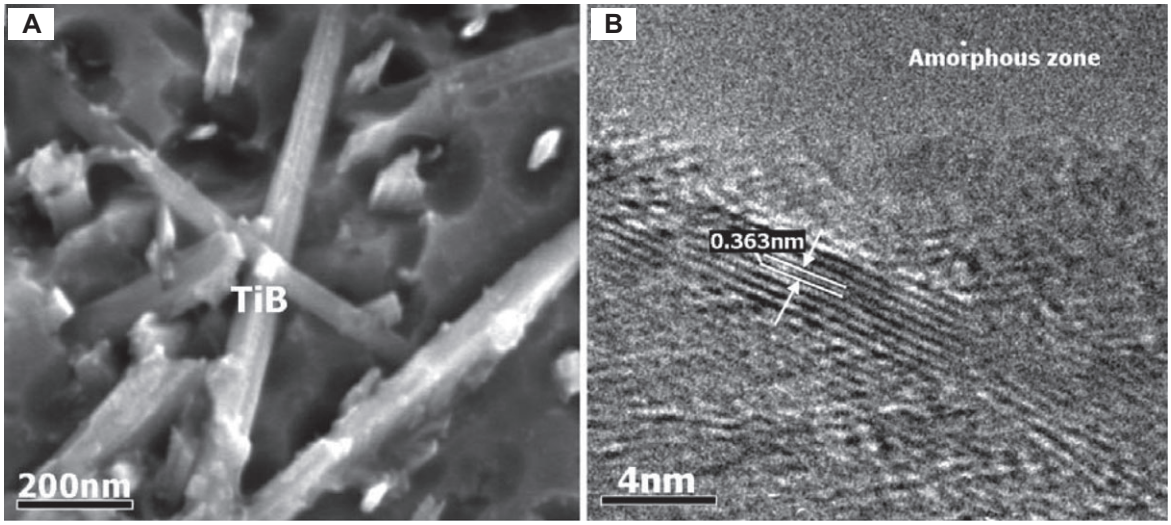

Figure 4 SEM micrograph (A), and the HREM morphologies (B) of TiB.

In fact, due to the dilution effect of the substrate on the coating, a great number of Ti entered into the molten pool from the substrate. The bottom of the coating was nearest to the substrate, so the Ti density was the largest in this location, which was favorable to the production of TiB. As shown in Figure 4A, the stick-shape TiB precipitates were produced in the coating. The HREM analysis result indicated that the TiB high-resolution lattice phase was produced in the alloying layer, which corresponded to its (101) crystal plane (see Figure 4B). The formations of the stick-shape TiB precipitates were mainly attributed to the lattice characteristics of TiB, which may act as the heterogeneous nucleation of the matrix phase [10]. As mentioned previously, a Ti-rich molten pool was produced in this sample. Thus, a large quantity of the TiB phases was produced in the composite coating. Moreover, also as shown in Figure 4B, the HREM irregular lattice fringe also indicated that the amorphous phase was present in the alloying layer. In fact, laser alloying is one of the surface amorphization technologies due to the sufficiently rapid heating and cooling that inhibits long-range diffusion and avoids crystallization [11]. There is a series of amorphous alloying with high glass forming ability in Zr-based alloy systems. A number of Zr played an important role in producing the amorphous alloys, which was beneficial in improving the wear resistance of the composite coating [12].

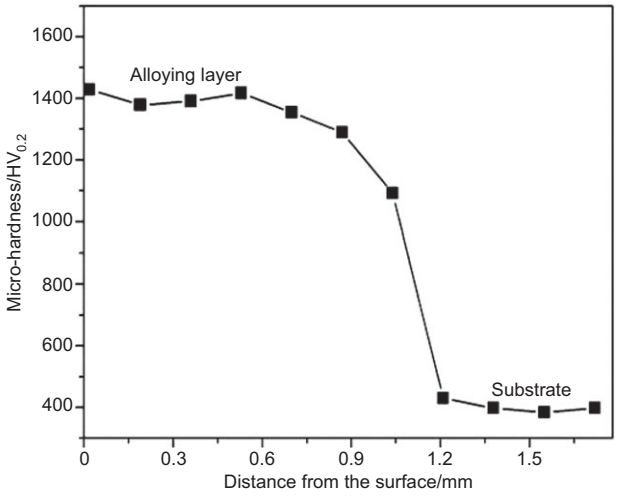

Figure 5 Microhardness distribution of the composite coating in the sample.

3.3 Microhardness and wear resistance

Under the actions of the phase constituent, the fine grain strengthening and the solution strengthening, the microhardness of the composite coating was in the range of 1350~1430 $HV_{0.2}$, which was approximately three to four times higher than that of the TA15 substrate (about 390 $HV_{0.2}$) (see Figure 5).

When the load was 54 N, SEM micrographs showed the worn surface of the TA15 alloy. It was also noted that serious adhesion patches, deep plowing grooves were present in the worn surface (see Figure 6A). Owing to its lower microhardness, under the action of the counterpart, a part of the TA15 alloy can be easily peeled off, leading to the formations of the adhesion patches. However, due to the action of the high microhardness of the composite coating, the hard asperities on the surface of the counterpart had difficulty penetrating it, leading to the improvement of the wear properties, which prevented the formations of the adhesion

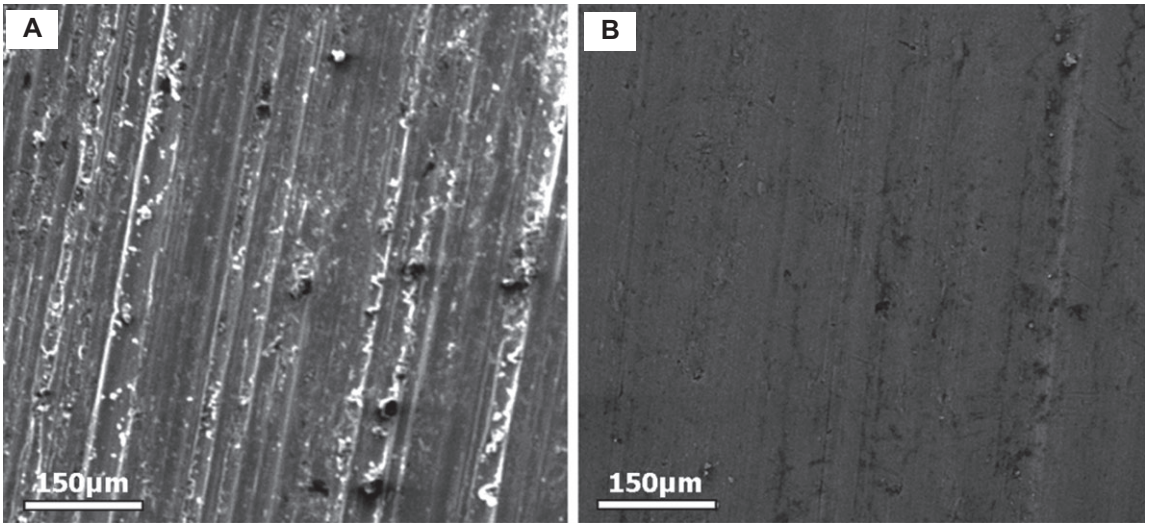

Figure 6 Worn morphologies of the TA15 substrate (A) and the composite coating (B).

patches and deep plowing grooves (see Figure 6B). Furthermore, under the dry-sliding wear test, the moderate growth dispersal precipitates, such as titanium borides, $TiC_{0.3}N_{0.7}$ and $Mo_5(Si, Al)_3C$, may withstand the external normal load better, leading to the improvement of the wear resistance [13]. Moreover, the productions of the amorphous alloys also decreased the wear volume loss of the composite coating. The wear volume loss of TA15 substrate was approximately six times higher than that of the composite coating.

4 Conclusions

The correct choice of the laser alloying parameters provides the Co-Fe-Al+B_4C-Si_3N_4 laser alloying composite coating on TA15 titanium alloy with the microhardness distribution in the range of 1350~1430 $HV_{0.2}$, which was approximately three to four times higher than that of the TA15 substrate (about 390 $HV_{0.2}$). This composite coating mainly consisted of γ-Co, TiB_2, TiB, $TiC_{0.3}N_{0.7}$, SiC, Ti_3Al, FeAl, and Co-Ti intermetallics. The diffraction pattern indicated that the orientation relationship between TiB_2 and $TiC_{0.3}N_{0.7}$ was $(\bar{1}20)TiB_2//(\bar{2}20)TiC_{0.3}N_{0.7}$ in the composite coating. Furthermore, during the alloying process, a number of Mo and Zr entered into the molten pool from the substrate, which refined the microstructures and also increased the amorphous phase content in the composite coating. The wear volume loss of the composite coating was approximately six times less than that of TA15 titanium alloy.

Acknowledgements: This work was financially supported by the Scientific Research Project of Shandong Jiao'tong University (Z201126).

Received June 1, 2012; accepted July 16, 2012; previously published online September 4, 2012.

References

[1] Wang HM, Qi JQ, Zou CM, Wei ZJ. *Mater. Sci. Technol.* 2012, 28, 597–602.
[2] Vaziri A, Shahverdi HR, Shabestari SG, Torkamany MJ. *Mater. Sci. Technol.* 2009, 25, 1234–1237.
[3] Alemohammad H, Esmaeili S, Toyserkani E. *Mater. Sci. Eng.* 2007, 456, 156–161.
[4] LiangB YH, Wang HY, Yang YF, Du YL, Jiang QC. *Int. J. Refract. Met. Hard Mater.* 2008, 26, 383–388.
[5] Ozyurek D, Ibrahim C. *Sci. Eng. Compos. Mater.* 2011, 1–2, 6–12.
[6] Ozyurek D, Tekeli S. *Sci. Eng. Compos. Mater.* 2010, 1, 31–38.
[7] Yang RJ, Liu ZD, Yang G, Ren WY. *Procedia Eng.* 2012, 36, 355–359.
[8] Lusquinos F, Pou J, Quintero F, Perez-Amor M. *Surf. Coat. Technol.* 2008, 202, 1588–1593.
[9] Kooi BJ, Pei YT, de Hosson JTM. *Acta Mater.* 2003, 51, 831–845.
[10] Wang YF, Li G, Wang CS, Xia YL, Sandip B, Dong C. *Surf. Coat. Technol.* 2004, 176, 284–289.
[11] Wu XL, Hong YS. *Surf. Coat. Technol.* 2001, 141, 141–144.
[12] Wang CS, Chen YZ, Li T, Yao B. *Appl. Surf. Sci.* 2009, 256, 1609–1613.
[13] Zhu QS, Shobu K. *J. Eur. Ceram. Soc.* 2000, 20, 1385–1389.